Development of low pH cement systems forming magnesium silicate hydrate (M-S-H)

Tingting Zhang [a,b], C.R. Cheeseman [a,*], L.J. Vandeperre [b]

[a] Department of Civil and Environmental Engineering, Imperial College London, South Kensington Campus, London SW7 2AZ, United Kingdom
[b] Centre for Advanced Structural Ceramics, Department of Materials, Imperial College London, South Kensington Campus, London SW7 2AZ, United Kingdom

ABSTRACT

This work aimed to develop novel cement systems for waste encapsulation that would form with a pH of around 10. The approach taken was to investigate the formation of brucite by hydration of a light burned periclase (MgO). Commercially available MgO powders often contain some CaO, and therefore silica fume was added to form C-S-H gel. Identification of the hydrated phases in MgO/silica fume samples showed that brucite formed in substantial quantities as expected. However, brucite reacted with the silica fume to produce a magnesium silicate hydrate (M-S-H) gel phase. After 28 days, the pH of systems rich in MgO tended towards the pH controlled by residual brucite (~10.5), whereas when all brucite reacts with silica fume a cement with an equilibrium pH just below 10 was achieved.

© 2011 Elsevier Ltd. All rights reserved.

1. Introduction

Cements are widely used for waste encapsulation to limit contaminant mobility [1–8]. The cement forms a low permeability matrix and results in immobilisation of contaminants by incorporation into hydrated phases and by precipitation due to the prevailing pH in the pore solution [4]. The solubility of many heavy metals is low at around pH 10, and therefore cements with a pH in this range would be highly desirable for such applications. Such moderate pH cements are likely to be particularly desirable for nuclear waste management [9]. For example, in the UK there are significant quantities of mixed wastes containing both Mg and Al alloys. Whilst the high pH in Portland cement based binders passivates the corrosion of Mg alloys, Al alloys corrode under high pH conditions with evolution of H_2 gas. The pH range in which Al alloys show passive corrosion behaviour extends up to about pH 10 and therefore cements with equilibrium pore solutions in this pH range may balance the need for Mg alloy passivation whilst avoiding Al alloy corrosion.

The pH imposed by cement internally and on its environment is a function of the phases present. It follows that control of the pH is easier if the number of phases in the cement paste is limited. For example, the hydration of MgO is given by:

$$MgO + H_2O \rightarrow Mg^{2+} + 2OH^- \rightarrow Mg(OH)_2 \qquad (1)$$
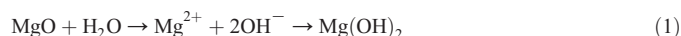
Magnesium hydroxide ($Mg(OH)_2$, brucite) is a useful starting point for the development of low pH cements because the pH of excess brucite in equilibrium with water is calculated readily from the solubility product of brucite to be around pH 10.5. Hence, in principle a cement based on the hydration of MgO powder, calcined at low temperature to ensure fast hydration, should yield a desirable pH.

However, most commercially available magnesium oxide powders contain some calcium oxide (lime, CaO) impurities. The presence of CaO has the potential to significantly increase the pH through dissolution of the oxide:

$$CaO + H_2O \rightarrow Ca^{2+} + 2OH^- \qquad (2)$$

Only when a pH of 12.5 is reached, will precipitation of calcium hydroxide ($Ca(OH)_2$) mitigate further increases in pH.

$$Ca^{2+} + 2OH^- \rightarrow Ca(OH)_2 \qquad (3)$$

A simple strategy to mitigate the pH increase due to the presence of CaO consists in adding a pozzolan capable of reaction with the Ca^{2+} ions or the calcium hydroxide ($Ca(OH)_2$, portlandite) formed during hydration of CaO, resulting in the formation of C-S-H gel. The aim of this paper was therefore to investigate whether mixtures of silica fume and commercial MgO could yield a pH close to 10.

2. Experimental methods

Blends of a commercially available MgO (MgO, MagChem 30, M.A.F. Magnesite B.V., The Netherlands) and silica fume (SF, Elkem Materials Ltd) were prepared. The chemical composition of the raw materials is reported in Table 1. Note that the MgO contains about 0.8 wt.% of CaO.

Table 1
Characteristics of the raw materials determined by the manufacturers.

	MgO	Silica fume
Composition		
SiO_2 (wt.%)	0.35	>97.5
Al_2O_3 (wt.%)	0.1	<0.7
Fe_2O_3 (wt.%)	0.15	<0.3
CaO (wt.%)	0.8	<0.3
P_2O_5 (wt.%)	(n/a)	<0.1
MgO (wt.%)	98.2	<0.5
K_2O (wt.%)	(n/a)	<0.6
Na_2O (wt.%)	(n/a)	<0.3
SO_3 (wt.%)	0.05	<0.4
Specific gravity (g cm^{-3})	3.23	1.94
Mean particle size (μm)[a]	5	21.3
BET surface area (m^2 g^{-1})	25	21.4

[a] Mass median diameter (D_{50}).

Fig. 1. Evolution with time of the pH for a blend of 50 wt.% MgO and 50 wt.% SF. Samples either remained in suspension throughout or the pH was measured by dispersing in water ground fragments of hydrated solid samples.

Two methods were used to study the pH evolution with time. In the first method, a paste of 50 wt.% MgO and 50 wt.% SF with water to solids ratio of 1 was prepared by adding a mixture of the solids to water and mixing the paste for 15 min. 100 g of the paste was then moulded into a rectangular tile and allowed to set and cure in sealed polyethylene bags. The pH was determined by crushing and grinding 1 g of sample and dispersing the fragments in 5 g of water. Following 24 h mixing, the solids were allowed to settle and the pH was measured by placing a standard glass pH electrode in the supernatant. In a second method, 10 g of a range of blends of MgO and silica fume was added to a polyethylene cylindrical container containing 100 g of distilled water. The tubes were sealed and agitated by device rotation (10 rpm). For pH measurements, the solid particles in these suspensions were allowed to settle determining the pH of the supernatant. For both methods the samples were kept in a laboratory where the temperature was controlled to 23 ± 1 °C.

The hydration products of samples cured in polyethylene bags were investigated using X-ray diffraction (XRD, Philips PW1720 powder diffractometer with a Cu Kα source). This information was then used to guide predictions of the pH made using Visual MINTEQ 2.6 [10], a windows implementation of the MINTEQA2 algorithm [11] for calculation of geochemical aqueous equilibrium to interpret the results of the pH study. The equilibrium constants of the formation reactions for the species considered have been summarised in Table 2.

To clarify some of the XRD data obtained, pure M-S-H gel was synthesised according to the method described by Brew and Glasser [12]. Solutions of $Na_2SiO_3 \cdot 5H_2O$ and $Mg(NO_3)_2 \cdot 6H_2O$ were cooled at 0 °C and mixed by stirring in a three-necked flask at a 1:1 Mg/Si ratio with the flask kept immersed in an ice-water bath during the precipitation process. The $Na_2SiO_3 \cdot 5H_2O$ was initially added followed by the $Mg(NO_3)_2 \cdot 6H_2O$. The precipitated composite was filtered and washed to remove all Na^+ ions. The solid part was then dried in a desiccator at 20 °C for 7 days.

3. Experimental results

Fig. 1 shows that the pH evolution with time for both test methods is essentially the same. The agreement between the two methods was
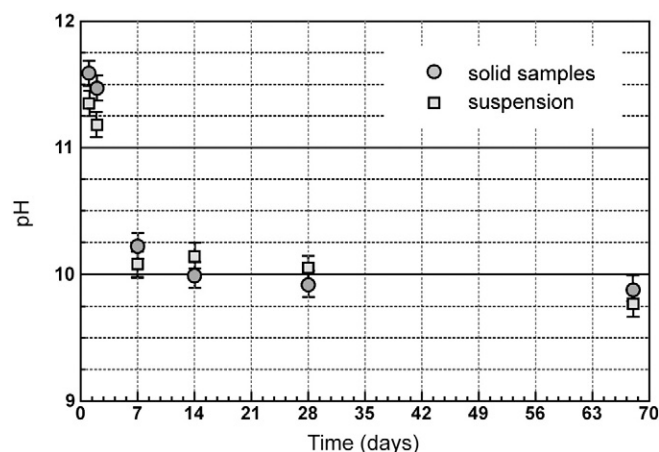
also observed for a much wider range of blends of MgO, Portland cement, metakaolin, blast furnace slag and silica fume [13], and confirms that the much easier method of using suspensions rather than pastes gives a good indication of the pH in this system. Fig. 2 shows the variation of pH with composition for blends of MgO and SF after 7 and 28 days. The following points can be observed:

(i) The pH of the suspensions containing only silica fume or only MgO hardly changes over 28 days. In fact, even when these measurements were extended to 63 days, the pH of the suspension containing only silica fume had decreased by only 0.08, and the pH of the suspensions containing only MgO had changed by only 0.02.

(ii) After 7 days, mixtures with less than 50 wt.% SF have a higher pH than mixtures with more than 50 wt.% SF;

(iii) and after 28 days the pH of most mixtures decreased relative to the 7 day value and mixtures with a higher SF content still show lower pH values than mixtures with a low SF content.

Fig. 3 shows XRD data after 7 and 28 days for two blends: one containing 50 wt.% SF and 50 wt.% MgO and one containing 80 wt.% SF and 20 wt.% MgO. For both types of blends little or no XRD signal for the original MgO remains after 7 days. Brucite is the main crystalline phase, and this is consistent with observations elsewhere when a MgO powder of similar reactivity is exposed to water [14]. After 28 days, brucite is present in samples with 50 wt.% MgO, but is not present in samples with 20 wt.% MgO in which only poorly crystalline phases remain. The amorphous phases give broad peaks at 18–25° 2θ, 32–37° 2θ and 58–62° 2θ. Comparison with the XRD data of fused silica and pure magnesium silicate hydrate gel (M-S-H), also shown in Fig. 3, shows that these broad peaks can only in part be explained by the presence of SF, and that the broad peaks in the 32–37° 2θ and the 58–62° 2θ regions are consistent with the characteristic XRD data of magnesium silicate hydrate (M-S-H) gel. Hence, brucite and SF have reacted to form M-S-H gel.

Table 2
Thermodynamic data used for pH predictions.

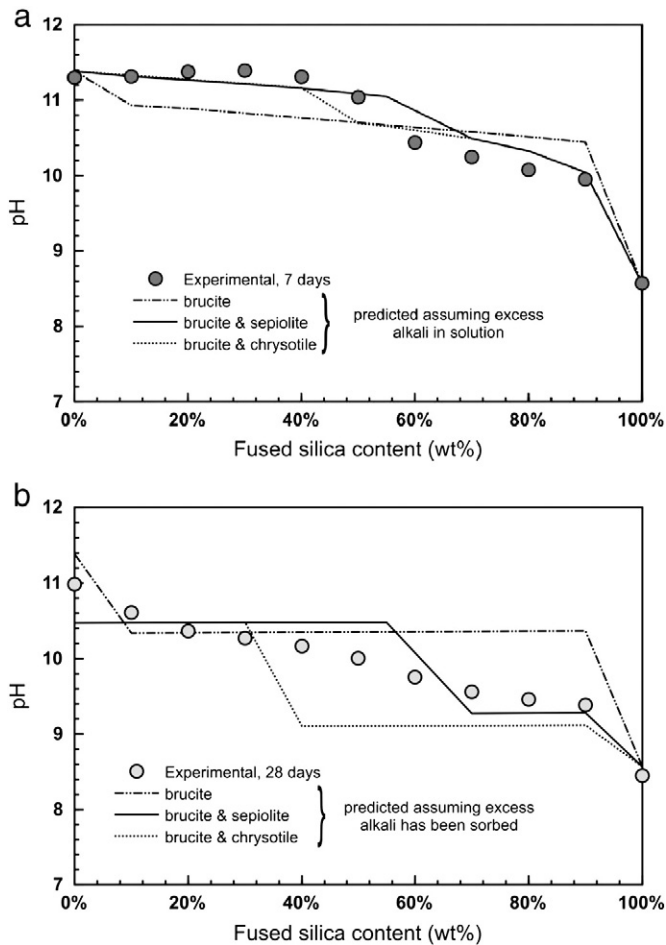| Species	Formation reaction	Log K	Ref.
Quartz	$H_4SiO_4 \rightarrow SiO_2 + 2H_2O$	4	[12]
Brucite	$Mg^{2+} + 2H_2O \rightarrow Mg(OH)_2 + 2H^+$	−17.1	[23]
Periclase	$Mg^{2+} + H_2O \rightarrow MgO + 2H^+$	−21.584	[12]
Chrysotile	$3Mg^{2+} + 2H_4SiO_4 + H_2O \rightarrow Mg_3(Si_2O_5)(OH)_4 + 6H^+$	−32.2	[12]
Sepiolite	$2Mg^{2+} + 3H_4SiO_4 \rightarrow \frac{1}{2}(Mg_4(Si_2O_5)_3(OH)_2 \cdot 6H_2O) + 4H^+ + \frac{1}{2}H_2O$	−15.76	[12]

Fig. 2. Variation of pH with composition when 10 g of MgO/SF blends were dispersed in 100 g of distilled water measured after (a) 7 days and (b) 28 days.
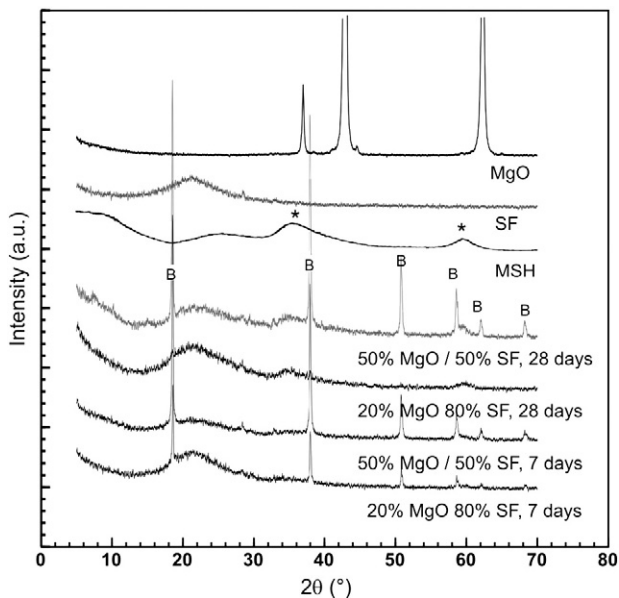

Fig. 3. XRD data of the raw materials (MgO and SF) and blends containing 50 wt.% MgO/50 wt.% SF or 20 wt.% MgO/80 wt.% SF, after 7 and 28 days of hydration. The appearance of a broad peak in the blends not seen in SF is indicated with an asterisk (*). The peak positions for brucite are indicated as B.

4. Results of pH calculations

When MgO is added to water, it will dissolve according to:

$$MgO + 2H^+ \rightarrow Mg^{2+} + H_2O \tag{4}$$

This raises both the pH and the Mg^{2+} concentration in solution. Once the Mg^{2+} concentration is raised above the concentration in equilibrium with magnesium hydroxide (brucite, $Mg(OH)_2$), magnesium hydroxide should precipitate according to:

$$Mg^{2+} + 2OH^- \rightarrow Mg(OH)_2 \tag{5}$$

Eventually all MgO should dissolve and precipitate as brucite. Moreover, since brucite dissolution and precipitation are known to be rapid [15], the pH should not rise significantly above the value for brucite (pH ~ 10.5). Experimentally, however, the pH was measured to be 11.3 and remained stable at this value even after 60 days. This cannot be due to the MgO itself and indicates an excess of alkaline impurities, which dissolve from the MgO powder. CaO is a common contaminant of MgO samples and is the major impurity in the commercially available MgO used in this work, as shown in Table 1. Therefore the presence of such excess alkalis in the raw material was modelled by replacing a small amount of the MgO with CaO so that a pH of 11.3 is reached at the experimental solids loading of 100 g L^{-1}. The level of CaO needed was only 0.078 wt.%.

Similarly, addition of SF is not expected to cause an increase in pH from 7, whereas experimentally a pH of 8.3 was measured. Again this indicates the presence of excess alkali in this industrial material, consistent with the reported composition data in Table 1. The excess alkali content of the silica fume was also modelled as a small amount of CaO replacing SiO_2. In this case, the CaO content needed to explain the pH was only 0.00024 wt.%.

A first step in the actual analysis then consisted of mixing the modified raw materials and adding them at a concentration of 100 g/L to water. The prediction for the pH assuming only brucite can form is shown in Fig. 2a. This clearly does not confirm the experimental data. Also shown in Fig. 2a is the predicted pH when it is assumed that either sepiolite, a typical formula for which is $Mg_4Si_6O_{15}(OH)_2 \cdot 6H_2O$, or chrysotile ($Mg_3(Si_2O_5)(OH)_4$) can form in addition to brucite. These crystals were selected as their Mg to Si ratios are very similar to the values measured by Brew and Glasser for M-S-H gel [12]. Amorphous phases are typically more soluble than crystalline phases, but it is clear that the overall trend in pH results is reproduced quite accurately. The experimental transition between lower and higher pH values (~ 55 wt. % SF) is in between the transition compositions for pure chrysotile and sepiolite. This is again consistent with the findings of Brew and Glasser as M-S-H gel was found to form with Mg/Si ratio between 0.67 and ~1. This is between the Mg/Si ratios of chrysotile (Mg/Si 1–1.5) and sepiolite (Mg/Si 0.67).

The predictions shown in Fig. 2b for the pH results after 28 days are essentially the same as those made for 7 days, except that the excess alkali has now been removed for all compositions except the end members. It can be seen that this leads to a pH dominated by the presence of brucite in mixtures rich in MgO, whereas the brucite is predicted to react fully at high SiO_2 contents yielding a pH ~9. As discussed above, the experimental transition between these two regions is more gradual for the amorphous M-S-H gel than that predicted for the pure crystalline materials.

This suggests that the reduction in pH during ageing is due to sorption or precipitation of alkali impurities. In the case of Ca, this can be explained by the formation of calcium silicate hydrate gel (C-S-H) as intended or by carbonation. If other alkali ions are present, then these probably are absorbed by the gels as both C-S-H and M-S-H gels have been reported to adsorb alkali metal ions [16].

5. Discussion

The hypothesis that mixing MgO with SF would yield a cement with an extractable pH ~10.5 has been confirmed. Mixtures which contain mostly MgO form excess brucite, which then governs the pH. Moreover, the higher initial pH, related to impurities in the feedstock materials, can indeed be overcome either by formation of C-S-H gel, carbonation or by adsorption of alkalis in C-S-H or M-S-H gels.

The pH calculations reported here were made at concentration of solids in the experimental pH measurements, and therefore was much more dilute than in the actual cement paste. Hence, the effect of highly soluble impurities on pH will have been diluted and pH values in the pore solution will be higher. However, in terms of the predictions without impurities and therefore also for more mature cement mixtures, the effect of dilution will have been much more limited: silica, brucite and M-S-H gel are low solubility phases and as long as the same solid phases remain present in excess, the same pH will be imposed.

The relative ease of formation of M-S-H gel was not expected, although this does agree with previous observations [17]. Moreover, both the pH versus composition and the XRD results are quite clear that M-S-H gel has formed. This is different from earlier work by Vandeperre et al. [14,18,19] on reactive MgO cements where MgO was mixed with pulverised fuel ash, which contains substantial amounts of soluble silica. In this previous work brucite remained present, and whilst some hydrotalcite was formed, there was no evidence for any M-S-H gel formation. Brew and Glasser [16] hypothesised that M-S-H gel may form during hydration of slag blends and that this might explain their ability to retain K. In fact, most documented cases of M-S-H gel formation are as part of the end product of magnesium sulphate attack on Portland cement [20].

The fact that M-S-H gel forms so readily suggests a route to production of cement with an equilibrium pH closer to 9.5 providing a high enough SF content is used so that all brucite is converted into M-S-H gel. The fact that some brucite remains at 28 days for samples with only 50 wt.% SF (molar Mg/Si ratio of 1.5) is consistent with the results of Brew and Glasser that M-S-H gels with a molar Mg/Si ratio greater than 1.0 did not form.

Early experimental results on the mechanical properties achievable with this type of cement are encouraging and compressive strength values up to 70 MPa at 28 days have been achieved [21], which suggests these systems may be useful for waste encapsulation.

6. Conclusions

Silica fume (SF) additions to MgO allow the effect of alkali impurities to be countered so that the pH of water in equilibrium with the cement will tend to 10.5, as expected for brucite.

Identification of the hydration phases in mixes of MgO and SF showed that in addition to brucite, a hydrated magnesium silicate (M-S-H) gel formed by reaction of the brucite and the SF.

The formation of M-S-H gel was confirmed by comparison with synthetic M-S-H gel and by modelling the pH versus composition using crystalline magnesium silicates as a surrogate for the M-S-H gel.

High MgO contents do not affect the pH, whereas high SF contents result in a pH closer to 9.5. Both types of composition have potential applications for the encapsulation of metal containing wastes.

References

[1] M. Yousuf, A. Mollah, R.K. Vempati, T.C. Lin, D.L. Cocke, The interfacial chemistry of solidification stabilization of metals in cement and pozzolanic material systems, Waste Manage 15 (1995) 137–148.
[2] R.D. Spence, Stabilization of high salt waste using a cementitious process, Innovative Technology Summary Report, Department of Energy, USA, 1999.
[3] J. Paya, M.V. Borrachero, J. Monzo, M. Bonilla, Properties of Portland cement mortars incorporating high amounts of oil–fuel ashes, Waste Manage 19 (1999) 1–7.
[4] B. Batchelor, Overview of waste stabilization with cement, Waste Manage 26 (2006) 689–698.
[5] C.M. Jantzen, Radioactive waste—Portland cement systems: II. Leaching characteristics, Journal of the American Ceramic Society 67 (1984) 674–676.
[6] C.M. Jantzen, F.P. Glasser, E.E. Lachowski, Radioactive waste—Portland cement systems: I. Radionuclide distribution, Journal of the American Ceramic Society 67 (1984) 668–673.
[7] S. Asavapisit, G. Fowler, C.R. Cheeseman, Solution chemistry during cement hydration in the presence of metal hydroxide wastes, Cement and Concrete Research 27 (1997) 1249–1260.
[8] J.R. Fitch, C.R. Cheeseman, Characterisation of environmentally exposed cement-based stabilised/solidified industrial waste, Journal of Hazardous Materials 101 (2003) 239–255.
[9] N.B. Milestone, Reactions in cement encapsulated nuclear wastes: need for toolbox of different cement types, Reactions in cement encapsulated nuclear wastes: need for toolbox of different cement types 105 (2006) 13–20.
[10] J.P. Gustafsson, Visual MINTEQ, KTH, Dept. of Land and Water Resources Engineering, Stockholm, 2009.
[11] J.D. Allison, D.S. Brown, K.J. Novo-Gradac, MINTEQA2/PRODEFA2 A geochemical assessment model for environmental systems, U.S. Environmental Protection Agency, 1991.
[12] D.R.M. Brew, F.P. Glasser, Synthesis and characterisation of magnesium silicate hydrate gels, Cement and Concrete Research 35 (2005) 85–98.
[13] T. Zhang, C.R. Cheeseman, L.J. Vandeperre, Development of novel low pH cement systems for encapsulation of wastes containing aluminium, Decommissioning, Immobilisation and Management of Nuclear Waste for Disposal 2009, York, 2009.
[14] L.J. Vandeperre, M. Liska, A. Al-Tabbaa, Microstructures of reactive magnesia cement blends, Cement and Concrete Composites 30 (2008) 706–716.
[15] O.S. Pokrovsky, J. Schott, Experimental study of brucite dissolution and precipitation in aqueous solutions: surface speciation and chemical affinity control, Geochimica Et Cosmochimica Acta 68 (2004) 31–45.
[16] D.R.M. Brew, F.P. Glasser, The magnesia-silica gel phase in slag cements: alkali (K, Cs) sorption potential of synthetic gels, Cement and Concrete Research 35 (2005) 77–83.
[17] J.X. Wei, Y.M. Chen, Y.X. Li, The reaction mechanism between MgO and microsilica at room temperature, Journal of Wuhan University of Technology-Materials Science Edition 21 (2006) 88–91.
[18] L.J. Vandeperre, M. Liska, A. Al-Tabbaa, Mixtures of pulverized fuel ash, Portland cement and magnesium oxide: strength evolution and hydration products, in: M. Ilic, J.J.J.M. Goumans, S. Miletic, J.J.M. Heynen, G.J. Senden (Eds.), WASCON 2006, ISCOWA, Belgrade, Serbia, 2006, pp. 539–550.
[19] L.J. Vandeperre, M. Liska, A. Al-Tabbaa, Hydration and mechanical properties of magnesia. Pulverized fuel ash, and Portland cement blends, Journal of Materials in Civil Engineering 20 (2008) 375–383.
[20] J. Prasad, D.K. Jain, A.K. Ahuja, Factors influencing the sulphate resistance of cement concrete and mortar, Asian Journal of civil engineering (Building and housing) 7 (2006) 259–268.
[21] T. Zhang, L.J. Vandeperre, C.R. Cheeseman, MgO cement systems for the encapsulation of problematic nuclear wastes, Decommissioning, Immobilisation and Management of Nuclear Waste for Disposal 2010, Manchester, 2010.